2015 International Conference on Unmanned Aircraft Systems (ICUAS)
Denver Marriott Tech Center
Denver, Colorado, USA, June 9-12, 2015

Formation Flight Control of Multirotor Helicopters with Collision Avoidance

Ícaro Bezerra Viana, [1], icaro@ita.br
Igor Afonso Acampora Prado, [1], igorap@ita.br
Davi Antônio dos Santos,[1], davists@ita.br
Luiz Carlos Sandoval Góes,[1], goes@ita.br
[1] Instituto Tecnológico de Aeronáutica, Sao José dos Campos, Brazil 12228-900

***Abstract*—Among the main sub-areas covering the cooperative control problem of Unmanned Aerial Vehicles (UAVs), formation flight has attracted great interest and has been widely investigated. The main purpose of the formation flight control is to establish a desired shape of formation for a group of vehicles by controlling the positions of each vehicle. The present paper deals with the problem of position formation flight control of a group of three multirotor helicopters with collision avoidance. In order to solve the problem, we propose a decentralized scheme based on model predictive controllers (MPC) for formation according to a virtual structure approach. For collision avoidance, a set of convex constraints on the vehicle's positions are included. The proposed method is evaluated on the basis of computational simulations considering that the vehicles are subject to disturbance forces. Simulation results show the effectiveness of the method with primary focus on treatment of anti-collision constraints.**

I. Introduction

The multirotor-type unmanned aerial vehicle had become increasingly popular as robotic platforms due to its mechanical simplicity, dynamic capabilities, and suitability for use in both indoors and outdoors environments. Groups of cooperatives Unmanned Aerial Vehicles (UAVs) are of particular interest due to their ability to coordinate simultaneous coverage of large areas or cooperate in mapping tasks [1]. Specific applications include search and rescue, surveillance, communication, and traffic monitoring.

The collision prevention refers to non-collision between the cooperating vehicles of the formation, and requires that the aircraft or detect other using sensors or to report their positions to other vehicles. To ensure collision avoidance [2] uses an approach called mixed integer linear programming (MILP) for the trajectory planning of multiple UAVs where integer variables are added to the optimization process in order to deal with the constraints properly. Reference [3] also uses integer constraints on the problem formulation with the difference of using quadratic cost function resulting in a MIQP (mixed-integer quadratic program).

This paper presents a control system for flight in formation of multiple autonomous multirotors helicopters, adopting a virtual structure configuration. In this, guiding the group of vehicles is easier than in other configurations, since all the agents of the formation are treated as a single object [4]. In order to ensure, simultaneously, performance in the trajectory tracking and treating the collision avoidance constraints between vehicles, a structure with MPC controllers is used for guiding the vehicles. In this, the design of a position controller is replicated for each vehicle that composed the formation, consisting of a linear state-space model predictive control (MPC) strategy. Thus, is used here the trajectory control proposed in [5], where the controller is designed taking into account a conical constraint on the total thrust vector, ie constraints on the inclination of the rotor plane and on the magnitude of the total thrust vector. This paper extends the problem treated in [5] and [6] including a set of linear and convex constraints to treat the collision avoidance problem in a simplified manner.

Figure 1 shows the block diagram with the architecture composed of three model predictive controllers (MPC) to the formation control, where each controller is capable to controlling only the three-dimensional position $r^{(i)} \in \mathbb{R}^3$ of a multirotor helicopter to follow a time-varying position command $\bar{r}^{(i)} \in \mathbb{R}^3$, where i denotes the i^{th} vehicle. To implement the set of constraints in the MPC is assumed that the vehicles can communicate with each other, so that each vehicle position information is passed on to neighboring vehicles of the formation. The variable $\bar{\rho}_{(ij)}$ are the increment for the desired position of the vehicle j in relation to the vehicle i, $\forall i \neq j$.

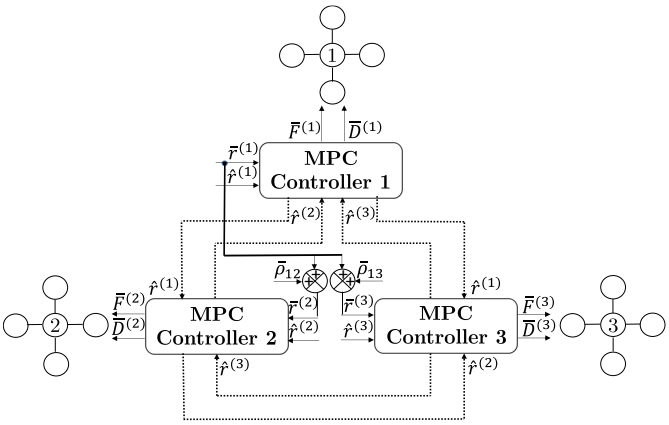

Fig. 1. Block diagram of a formation flight control for three multirotors.

The control system for each multirotor is composed of an outer loop represented by the MPC for position control, and a inner loop for attitude control. In the Figure 1 in the part that represents the vehicle is implicitly the existence of an attitude control block that receives an attitude command $\bar{D} \in \mathrm{SO}(3)$. The command for the total thrust magnitude $\bar{F} \in \mathbb{R}$ is generated by the outer loop of the system after the conversion of the control vector computed by the MPC. More details about the structure of the inner loop of the system is founded in [5].

This research was conducted in the scope of the Aerial Robotics Laboratory (LRA) located at the Technological Institute of Aeronautics (ITA), as illustrated in Figure 2, which has a research group in the field of aerial robotics. The present laboratory have three aerial vehicles: two quadrotors and an octo-rotor. Moreover, a software in the loop (SIL) and a flight test environment are being designed.

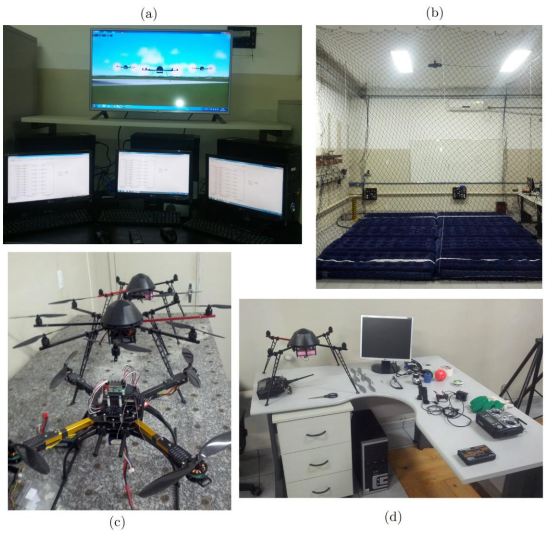

Fig. 2. Aerial robotics research in LRA-ITA.

The rest of the body text is organized as follows: Section II presents the definition of the problem. Section III describes the problem solution. Section IV describes the evaluation based on computer simulations using MATLAB/SIMULINK and Section V contains the conclusions and suggestions for future work.

II. Problem Statement

Consider the multirotor vehicle and the three Cartesian coordinate systems (CCS) illustrated in Figure 3. It is assumed that the vehicle has a rigid structure. The body CCS $S_{\mathrm{B}} \triangleq \{X_{\mathrm{B}}, Y_{\mathrm{B}}, Z_{\mathrm{B}}\}$ is fixed to the structure and its origin coincides with the center of mass (CM) of the vehicle. The reference CCS $S_{\mathrm{R}} \triangleq \{X_{\mathrm{R}}, Y_{\mathrm{R}}, Z_{\mathrm{R}}\}$ is Earth-fixed and its origin is at point O. Finally, the CCS $S_{\mathrm{R}'} \triangleq \{X_{\mathrm{R}'}, Y_{\mathrm{R}'}, Z_{\mathrm{R}'}\}$ is defined to be parallel to S_{R}, but its origin is shifted to CM. Assume that S_{R} is an inertial frame.

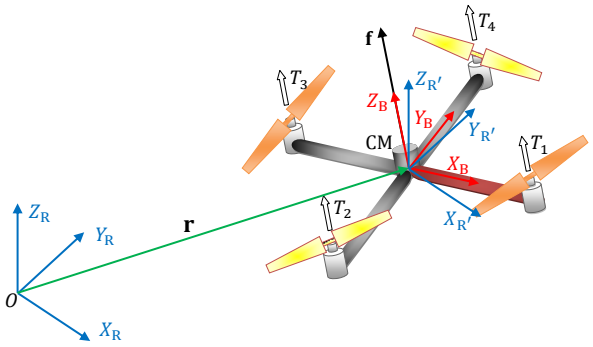

Fig. 3. The Cartesian coordinate systems.

Invoking the second Newton's law and neglecting disturbance forces, the translational dynamics of the multirotor illustrated in Figure 3 can be immediately described in S_{R} by the following second order differential equation:

$$\ddot{\mathbf{r}} = \frac{1}{m}\mathbf{f} + \begin{bmatrix} 0 \\ 0 \\ -g \end{bmatrix}, \tag{1}$$

where $\mathbf{r} \triangleq [r_{\mathrm{x}}\ r_{\mathrm{y}}\ r_{\mathrm{z}}]^{\mathrm{T}} \in \mathbb{R}^3$ is the position vector of CM, $\mathbf{f} \triangleq [f_{\mathrm{x}}\ f_{\mathrm{y}}\ f_{\mathrm{z}}]^{\mathrm{T}} \in \mathbb{R}^3$ is the total thrust vector, m is the mass of the vehicle, and g is the gravitational acceleration. As illustrated in Figure 3, $\mathbf{f}$ is perpendicular to the rotor plane.

Define the inclination angle $\phi \in \mathbb{R}$ of the rotor plane as the angle between Z_{B} and $Z_{\mathrm{R}'}$. The angle ϕ can thus be expressed by

$$\phi \triangleq \cos^{-1}\frac{f_{\mathrm{z}}}{f}, \tag{2}$$

where $f \triangleq \|\mathbf{f}\|$.

Define the position tracking error $\tilde{\mathbf{r}} \in \mathbb{R}^3$ as

$$\tilde{\mathbf{r}} \triangleq \mathbf{r} - \mathbf{r}_{\mathrm{d}}, \tag{3}$$

where $\mathbf{r}_{\mathrm{d}} \triangleq [r_{\mathrm{d,x}}\ r_{\mathrm{d,y}}\ r_{\mathrm{d,z}}]^{\mathrm{T}} \in \mathbb{R}^3$ is a position command.

Problem 1. Let $\phi_{\max} \in \mathbb{R}$ denote the maximum allowable value of ϕ, $f_{\min} \in \mathbb{R}$ and $f_{\max} \in \mathbb{R}$ denote, respectively, the minimum and maximum allowable values of f, and $\mathbf{r}_{\min} \in \mathbb{R}^3$ and $\mathbf{r}_{\max} \in \mathbb{R}^3$ denote, respectively, the minimum and maximum allowable values of $\mathbf{r}$. The problem is to find a control law for $\mathbf{f}$ that minimizes $\tilde{\mathbf{r}}$, subject to the inclination constraint $\phi \leq \phi_{\max}$, to the force magnitude constraint $f_{\min} \leq f \leq f_{\max}$, and to the position constraint $\mathbf{r}_{\min} \leq \mathbf{r} \leq \mathbf{r}_{\max}$.

Problem 2. Let a standalone controller referring to a i^{th} vehicle of the formation, a control action should calculate a command $\mathbf{f}^{(i)}$ so that $\mathbf{r}^{(i)}$, the current position of the vehicle (i), stay at a safety distance $\mathbf{D} \triangleq [d_{\mathrm{x}}\ d_{\mathrm{y}}\ d_{\mathrm{z}}]^{\mathrm{T}} \in \mathbb{R}^3$ in relation to $\mathbf{r}^{(j)}, \forall j \neq i$ at each time step, as show in Figure 4.

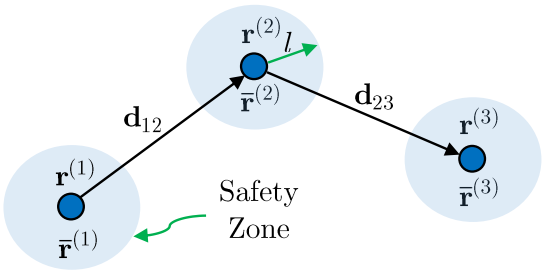

Fig. 4. Problem definition

In Figure 4 the variable l corresponds to the protection sphere radius of each vehicle and d_{ij} corresponds to the safety distances represented in the three-dimensional space. Thus, to ensure that these spheres do not collide, the minimum distance d_{ij} should be at least twice the sphere radius, where the value of l can be specified as the sum of the distance of the center of mass (CM) in relation to the rotor center, plus the length of the radius propeller.

It is assumed that, at each instant of time *k*, the multirotor (i) can get the information of vehicle position (j). Thus, to achieve the collision avoidance simply add the following set of linear inequality convex constraints,

$$If\ (\hat{r}_x^{(i)} - \hat{r}_x^{(j)}) > 0, \tag{4}$$

$$r_x^{(i)} - \hat{r}_x^{(j)} \geqslant d_{x_{ij}} \tag{5}$$

$$Otherwise,\ \hat{r}_x^{(j)} - r_x^{(i)} \geqslant d_{x_{ij}} \tag{6}$$

$$If\ (\hat{r}_y^{(i)} - \hat{r}_y^{(j)}) > 0, \tag{7}$$

$$r_y^{(i)} - \hat{r}_y^{(j)} \geqslant d_{y_{ij}} \tag{8}$$

$$Otherwise,\ \hat{r}_y^{(j)} - r_y^{(i)} \geqslant d_{y_{ij}} \tag{9}$$

$$If\ (\hat{r}_z^{(i)} - \hat{r}_z^{(j)}) > 0, \tag{10}$$

$$r_z^{(i)} - \hat{r}_z^{(j)} \geqslant d_{z_{ij}} \tag{11}$$

$$Otherwise,\ \hat{r}_z^{(j)} - r_z^{(i)} \geqslant d_{z_{ij}} \tag{12}$$

The notation $\hat{r}$ indicates a measured variable, with constant value, while $r^{(i)}$ is the manipulated variable of the optimization process that integrates the MPC controller.

III. Problem Solution

The solution to Problem 1 is based on a MPC strategy, described in more details in [5]. In short, the Problem 1 is solved using a linear state-space model predictive control whose optimization is made handy by replacing the original conic constraint set on the thrust vector by an inscribed pyramidal space, which rendered a linear set of inequalities.

This section proposes a solution to the Problem 2 by inserting linear convex constraints to the optimization problem. Subsection 3.1 describes the system by a discrete-time linear state-space model in the form of incremental control input.

A. Incremental-Input State-Space Model

Define the state vector $\mathbf{x} \triangleq [r_\mathrm{x}\ \dot{r}_\mathrm{x}\ r_\mathrm{y}\ \dot{r}_\mathrm{y}\ r_\mathrm{z}\ \dot{r}_\mathrm{z}]^\mathrm{T} \in \mathbb{R}^6$ and the control input vector $\mathbf{u} \triangleq [u_\mathrm{x}\ u_\mathrm{y}\ u_\mathrm{z}]^\mathrm{T} \in \mathbb{R}^3$

$$\mathbf{u} \triangleq \frac{1}{m}\mathbf{f} - \begin{bmatrix}0\\0\\g\end{bmatrix}. \tag{13}$$

Using equation (13), (1) can be immediately rewritten as a continuous-time linear state-space model

$$\dot{\mathbf{x}} = \mathbf{A}\mathbf{x} + \mathbf{B}\mathbf{u}, \tag{14}$$

with

$$\mathbf{A} = \begin{bmatrix}0&1&0&0&0&0\\0&0&0&0&0&0\\0&0&0&1&0&0\\0&0&0&0&0&0\\0&0&0&0&0&1\\0&0&0&0&0&0\end{bmatrix} \in \mathbb{R}^{6\times6} \tag{15}$$

and

$$\mathbf{B} = \begin{bmatrix}0&0&0\\1&0&0\\0&0&0\\0&1&0\\0&0&0\\0&0&1\end{bmatrix} \in \mathbb{R}^{6\times3}. \tag{16}$$

Define the controlled output vector $\mathbf{y} \in \mathbb{R}^3$ to be the position vector, i.e.

$$\mathbf{y} \triangleq \mathbf{C}\mathbf{x}, \tag{17}$$

with

$$\mathbf{C} = \begin{bmatrix}1&0&0&0&0&0\\0&0&1&0&0&0\\0&0&0&0&1&0\end{bmatrix} \in \mathbb{R}^{3\times6}. \tag{18}$$

Let $\mathbf{x}(k) \in \mathbb{R}^6$, $\mathbf{u}(k) \in \mathbb{R}^3$, and $\mathbf{y}(k) \in \mathbb{R}^3$ denote, respectively, the state vector, the control input vector and the controlled output vector, all described in the discrete-time domain. Using the Euler integration method with an integration step of $T_s = 20$ ms, the discretized version of equation (14) and equation (17) is obtained as

$$\begin{array}{rcl}\mathbf{x}(k+1) &=& \mathbf{A}_\mathrm{d}\mathbf{x}(k) + \mathbf{B}_\mathrm{d}\mathbf{u}(k)\\ \mathbf{y}(k) &=& \mathbf{C}_\mathrm{d}\mathbf{x}(k)\end{array}, \tag{19}$$

where

$$\mathbf{A}_\mathrm{d} = \begin{bmatrix}1&0.02&0&0&0&0\\0&1&0&0&0&0\\0&0&1&0.02&0&0\\0&0&0&1&0&0\\0&0&0&0&1&0.02\\0&0&0&0&0&1\end{bmatrix} \in \mathbb{R}^{6\times6}, \tag{20}$$

$$\mathbf{B}_\mathrm{d} = \begin{bmatrix}0.0002&0&0\\0.02&0&0\\0&0.0002&0\\0&0.02&0\\0&0&0.0002\\0&0&0.02\end{bmatrix} \in \mathbb{R}^{6\times3}, \tag{21}$$

and $\mathbf{C}_\mathrm{d} \in \mathbb{R}^{3\times6}$ remains equal to $\mathbf{C}$.

Consider the discrete-time state-space model of equation (19). It can be rewritten in the incremental-input form as [9]

$$\begin{array}{rcl} \boldsymbol{\xi}(k+1) & = & \tilde{\mathbf{A}}\boldsymbol{\xi}(k) + \tilde{\mathbf{B}}\Delta\mathbf{u}(k) \\ \mathbf{y}(k) & = & \tilde{\mathbf{C}}\boldsymbol{\xi}(k) \end{array}, \tag{22}$$

with

$$\boldsymbol{\xi}(k) = \begin{bmatrix} \Delta\mathbf{x}(k) \\ \mathbf{y}(k) \end{bmatrix} \in \mathbb{R}^9, \tag{23}$$

$$\tilde{\mathbf{A}} = \begin{bmatrix} \mathbf{A}_\mathrm{d} & \mathbf{0}_{6\times3} \\ \mathbf{C}_\mathrm{d}\mathbf{A}_\mathrm{d} & \mathbf{I}_3 \end{bmatrix} \in \mathbb{R}^{9\times9}, \tag{24}$$

$$\tilde{\mathbf{B}} = \begin{bmatrix} \mathbf{B}_\mathrm{d} \\ \mathbf{C}_\mathrm{d}\mathbf{B}_\mathrm{d} \end{bmatrix} \in \mathbb{R}^{9\times3}, \tag{25}$$

and

$$\tilde{\mathbf{C}} = [\mathbf{0}_{3\times6} \quad \mathbf{I}_3] \in \mathbb{R}^{3\times9}, \tag{26}$$

where $\Delta\mathbf{x}(k) \triangleq \mathbf{x}(k) - \mathbf{x}(k-1) \in \mathbb{R}^6$ denotes the incremental state vector, $\Delta\mathbf{u}(k) \triangleq \mathbf{u}(k) - \mathbf{u}(k-1) \in \mathbb{R}^3$ is the incremental control input vector, $\mathbf{I}_3$ represents an identity matrix with dimensions 3×3, and $\mathbf{0}_{3\times6}$ is a matrix of zeros with dimension 3×6.

B. Prediction Model

Using equation (22), the prediction model can be obtained as (see [9], p.50)

$$\hat{\mathbf{y}}_N = \mathbf{G}\Delta\hat{\mathbf{u}}_M + \mathbf{F}, \tag{27}$$

where $\hat{\mathbf{y}}_N \in \mathbb{R}^{3N\times1}$ stacks the controlled outputs along a prediction horizon of length N, $\Delta\hat{\mathbf{u}}_M \in \mathbb{R}^{3M\times1}$ stacks the incremental control inputs along a control horizon of length M,

$$\mathbf{G} = \begin{bmatrix} \tilde{\mathbf{C}}\tilde{\mathbf{B}} & \mathbf{0}_{3\times3} & \dots & \mathbf{0}_{3\times3} \\ \tilde{\mathbf{C}}\tilde{\mathbf{A}}\tilde{\mathbf{B}} & \tilde{\mathbf{C}}\tilde{\mathbf{B}} & \dots & \mathbf{0}_{3\times3} \\ \vdots & \vdots & \ddots & \vdots \\ \tilde{\mathbf{C}}\tilde{\mathbf{A}}^{M-1}\tilde{\mathbf{B}} & \tilde{\mathbf{C}}\tilde{\mathbf{A}}^{M-2}\tilde{\mathbf{B}} & \dots & \tilde{\mathbf{C}}\tilde{\mathbf{B}} \\ \vdots & \vdots & & \vdots \\ \tilde{\mathbf{C}}\tilde{\mathbf{A}}^{N-1}\tilde{\mathbf{B}} & \tilde{\mathbf{C}}\tilde{\mathbf{A}}^{N-2}\tilde{\mathbf{B}} & \dots & \tilde{\mathbf{C}}\tilde{\mathbf{A}}^{N-M}\tilde{\mathbf{B}} \end{bmatrix} \in \mathbb{R}^{3N\times3M} \tag{28}$$

and

$$\mathbf{F} = \begin{bmatrix} \tilde{\mathbf{C}}\tilde{\mathbf{A}} \\ \tilde{\mathbf{C}}\tilde{\mathbf{A}}^2 \\ \vdots \\ \tilde{\mathbf{C}}\tilde{\mathbf{A}}^N \end{bmatrix} \boldsymbol{\xi}(k) \in \mathbb{R}^{3N}. \tag{29}$$

C. Collision Avoidance

Consider the following linear convex inequality constraint for the distances between the multirotors, according to (4-12),

$$\mathbf{r}^{(i)} - \hat{\mathbf{r}}^{(j)} \geqslant \mathbf{D} \tag{30}$$

The above constraints are employed in this work to avoid collisions between the vehicles (i) and (j), $\forall j \neq i$. The vector $\mathbf{D} \in \mathbb{R}^3$ corresponds to safety distances $d_{x_{ij}}, d_{y_{ij}}, d_{z_{ij}}$ in each direction of the vehicle. Repeating equation (30) along the prediction horizon N, yields,

$$\mathcal{Y}_N - [\hat{\mathbf{r}}^{(j)}]_N \geqslant [\mathbf{D}]_N. \tag{31}$$

which can be rewritten in terms of $\Delta\mathcal{U}_M$ using equation (27), providing,

$$\mathcal{A}\Delta\mathcal{U}_M \leqslant \gamma \tag{32}$$

where,

$$\mathcal{A} \triangleq [-\mathbf{G}] \in \mathbb{R}^{3N\times3M} \tag{33}$$

and,

$$\gamma \triangleq \left[-[\mathbf{D}]_N - [\hat{\mathbf{r}}^{(j)}]_N + \mathbf{F}\right] \in \mathbb{R}^{3N}. \tag{34}$$

which consists in the incremental form of the constraints on the controlled output of the i^{th} vehicle.

D. Model Predictive Controller

The optimal control vector $\mathbf{u}^*(k)$ computed at the discrete-time instant k is given by $\mathbf{u}^*(k) = \Delta\mathbf{u}^*(k) + \mathbf{u}^*(k-1)$, where $\Delta\mathbf{u}^*(k)$ is the first control vector of $\Delta\mathbf{u}^*_M$, which in turn is obtained by minimizing the following quadratic cost function:

$$J(\Delta\hat{\mathbf{u}}_M) = (\hat{\mathbf{y}}_N - [\mathbf{r}_\mathrm{d}]_N)^\mathrm{T}\,\mathbf{Q}\,(\hat{\mathbf{y}}_N - [\mathbf{r}_\mathrm{d}]_N) + \Delta\hat{\mathbf{u}}_M^\mathrm{T}\mathbf{R}\Delta\hat{\mathbf{u}}_M, \tag{35}$$

subject to the constraints (32).

In this work, the controlled output weighting matrix is assumed to be $\mathbf{Q} = \boldsymbol{\eta}\times\mathbf{I}_{3N}$ and the control input weighting matrix is assumed to be $\mathbf{R} = \boldsymbol{\rho}\times\mathbf{I}_{3M}$.

E. Computing Thrust Magnitude and Attitude Commands

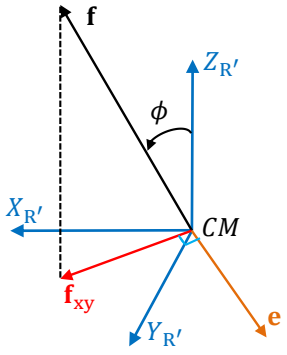

Fig. 5. Relation between the thrust vector $\mathbf{f}$ and its horizontal projection $\mathbf{f}_{xy}$.

In according to [6], after computation of the control input **u**, for implementation purposes, it is necessary to transform it into the corresponding commands of total thrust magnitude (throttle) f and attitude.

Rewrite equation (13) as

$$\begin{bmatrix} f_{\mathrm{x}} \\ f_{\mathrm{y}} \\ f_{\mathrm{z}} \end{bmatrix} = m \begin{bmatrix} u_{\mathrm{x}} \\ u_{\mathrm{y}} \\ u_{\mathrm{z}} + g \end{bmatrix}, \tag{36}$$

whose magnitude f is given by

$$f = m\sqrt{u_{\mathrm{x}}^2 + u_{\mathrm{y}}^2 + (u_{\mathrm{z}} + g)^2}, \tag{37}$$

which is the command for the magnitude of the total thrust $\bar{F}$.

The attitude commands $\bar{D}$ for the internal attitude control loop (see Figure 1) need to be computed from vector **f**, which has information about the orientation of the plane of rotors with respect the local horizontal. Note that there are infinite attitudes of S_{B} with respect to $S_{\mathrm{R}'}$ for which the Z_{B} axis coincides with **f**. In order to specify an unique attitude, it is necessary to select a heading angle. For example (since this work is not concerned with heading control), one can choose a zero heading angle, which is equivalent to just taking into consideration the attitude represented by the principal Euler angle/axis $(\phi, \mathbf{e})$, where ϕ is the inclination angle itself and the unit vector **e** (see Figure 5) is given by

$$\mathbf{e} = \frac{Z_{\mathrm{R}'} \times \mathbf{f}_{\mathrm{xy}}}{\|Z_{\mathrm{R}'} \times \mathbf{f}_{\mathrm{xy}}\|}, \tag{38}$$

where $\mathbf{f}_{\mathrm{xy}} \triangleq [f_{\mathrm{x}}\ f_{\mathrm{y}}]^{\mathrm{T}}$ denotes the horizontal projection of **f**. From $(\phi, \mathbf{e})$, this work represent the attitude of S_{B} with respect to S_{R} using direction cosine matrix (DCM) [10].

IV. Simulation Results

In this section, the proposed method is evaluated on the basis of computational simulations by using the MATLAB/SIMULINK software. The environment implemented containing a formation with a group of three multirotors helicopters adopting the Virtual Structure (VS) strategy. The selection of this formation configuration was due to the fact that not provide the error propagation to a neighboring vehicle when a subject vehicle undergoes a disturbance or external interference. Figure 6 shows the triangular formation used for testing the proposed scheme, which has a fixed-altitude plane. The vehicles maintain a straight line trajectory, where initially the vehicles 2 and 3 remain equidistant from the vehicle 1, resulting in an equilateral triangle. In this work, the choice of a simple trajectory was made because the goal here focus primarily on treatment of anti-collision constraints.

The decentralized scheme is composed of three computers connected by a network of Ethernet communication. Each computer contains a MPC controller and the dynamic model of the multirotor helicopter, and sends data via Ethernet of your position $\mathbf{r}^{(i)}$ for the others computers of the architecture. The exchange of position information is necessary in order to achieve the requirements of collision avoidance. Each computer is managed by the operating system Windows 7 Ultimate with Service Pack 1 and runs MATLAB/Simulink version 2012a. Figure 7 summarizes the configuration of the transmit data address used in the network.

TABLE I. Vehicle Parameters

Variables	Values
Vehicle mass, m	1 kg
Gravitational acceleration, g	9.81 m/s^2
Inertia I_x, I_y	1.71×10^{-2} kg m^2
Inertia I_z	2.86×10^{-2} kg m^2
Thrust factor	3.13×10^{-7}
Torque factor	7.5×10^{-7}
Lenght of arm, l	0.2 m

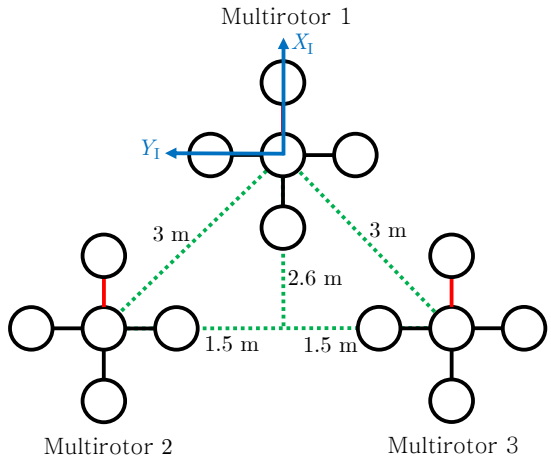

Fig. 6. Formation using the virtual structure approach

The 6DOF dynamics of each multirotor helicopter is simulated using the Runge-Kutta 4 as the solver with an integration step of 0.02s. The parameters of the platform is showed in Table I. In order to solve the optimization problem embedded in the MPC algorithm, the Interior-Point method is taken into account. The following parameterization is adopted for the controller. The control input weights and the controlled output weights are adjusted in $\boldsymbol{\rho} = [0.01\ 0.01\ 0.01]^{\mathrm{T}}$ and $\boldsymbol{\eta} = [1\ 1\ 1]^{\mathrm{T}}$, respectively. The prediction horizon and control horizon are set to $N = 80$ and $M = 5$, respectively. The maximum and minimum constraints on the force magnitude are set in $f_{\max} = 20$ N and $f_{\min} = 2$ N, respectively. Concerning the maximum inclination constraint ϕ_{max}, was adopted a value of 10°. The attitude controller are proportional-derivative laws tuned so as to make the attitude dynamics have a bandwidth significantly larger than the bandwidth of the position control dynamics.

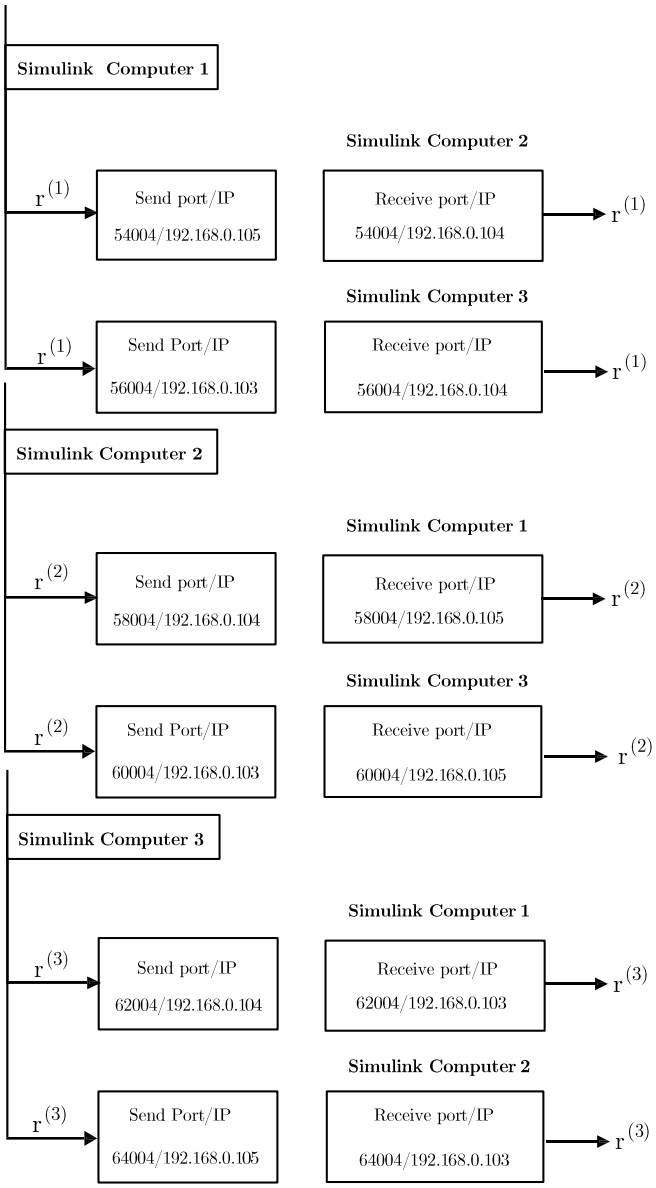

Fig. 7. Configuring the sending and receiving of $\mathbf{r}^{(i)}$.

Figure 8 shows the trajectory of vehicles leaving the following initial position in meters (m): $\mathbf{r}^{(1)} = [0\ 2\ 2]^{\mathrm{T}}$ m, $\mathbf{r}^{(2)} = [-2\ 2\ 2]^{\mathrm{T}}$ m, and $\mathbf{r}^{(3)} = [-4\ 2\ 2]^{\mathrm{T}}$ m. The three vehicles remains at the same altitude and have constant velocity motion in the longitudinal axis, this can been described by the following equations for the desired formation,

$$r_d(t) = [\lambda t\ r_{y_1}\ h]^{\mathrm{T}} \tag{39}$$

$$\rho_d^{(1)} = [0\ 0\ 0]^{\mathrm{T}} \tag{40}$$

$$\rho_d^{(2)} = [-\eta\ \tau\ 0]^{\mathrm{T}} \tag{41}$$

$$\rho_d^{(2)} = [-\eta\ (-)\tau\ 0]^{\mathrm{T}} \tag{42}$$

where $t \geq 0$ denotes the continuous time, $\lambda = 0.5$ m/s is the desired longitudinal speed performed by all platforms, $h = 2$ m is the altitude of the trajectory, $\eta = 2.6$ m is the longitudinal distance from the CM of the vehicle 1 to the CM of the other vehicles and $\tau = 1.5$ is the lateral distance between two neighboring vehicles.

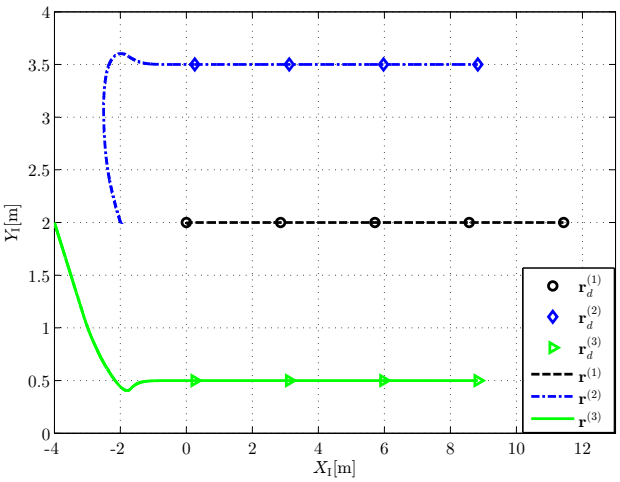

Fig. 8. Formation control without disturbances

To evaluate the efficiency of the controller to disturbance rejection was applied a lateral disturbance force in the vehicle 2 of $f_{d,y} = -1.2$ N and was observed the temporal response of the vehicle, as shown in Figure 9-(a). This magnitude value chosen for the disturbance force was applied on the input of the plant. It is observed that the vehicle is able to reject the disturbance. This is due to the incremental MPC formulation that give an integral action for the controller of the vehicle 2, allowing to track a constant set point with zero steady state error [9].

To validate that the collision avoidance requirement is attended, is showed in Figure 9-(b) the responses when the constraints in MPC of the vehicle 2 are active, considering that the same magnitude value of the disturbance force is applied on the system. It is possible to see the vehicle 2 satisfying a distance constraint equal to $\mathbf{D} = [0\ 1.45\ 0]^{\mathrm{T}}$ m in relation to the vehicle 1. Thus, rather than the vehicle 2 reaches $r_y = 3.4$ m as shown in Figure 9-(a), now it does not exceed $r_y = 3.45$ m, in order to respect the distance constraint $\mathbf{D}$.

In order to remove the vehicle 2 of its nominal trajectory and to illustrate the efficiency of the proposed method, a strong enough disturbance is applied to remove this vehicle of the formation as shown in Figure 10. Thus, to avoid the collision between the vehicles 1 and 2 was used an anti-collision constraint with value to the safety distance $\mathbf{D} = [0\ 1\ 0]^{\mathrm{T}}$ m. It is seen, in Figure 10-(a), that the MPC controller operates such that the safety distance is maintained. Figure 10-(b) shows the relative distance between the vehicles 1 and 2 where can be seen that the collision avoidance is achieved.

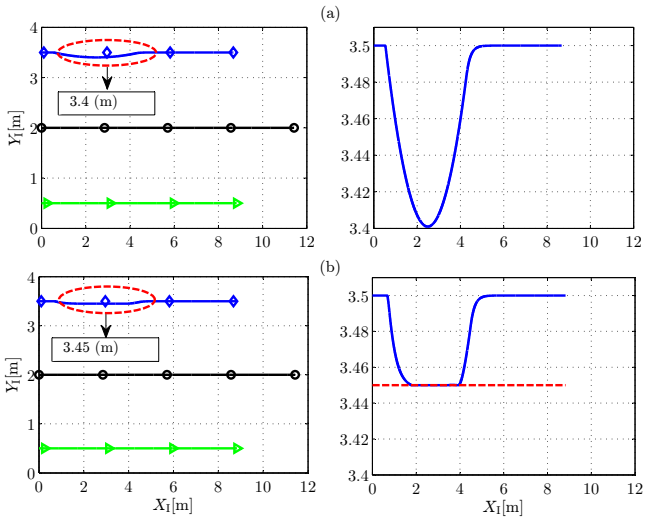

Fig. 9. Collision avoidance acting in vehicle 2 with disturbance.

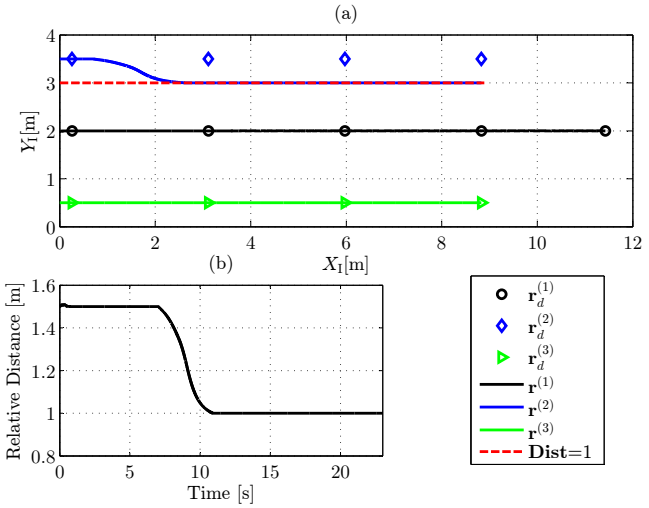

Fig. 10. (**a**) Collision avoidance constraint acting in the vehicles. (**b**) Relative distance between vehicles 1 e 2.

Finally, is illustrated a example where a disturbance is applied in a vehicle that the constraints in MPC are inactive, and it is analized the neighbor vehicles that have active the collision avoidance constraints. The initial conditions are now: $\mathbf{r}^{(1)} = [0\ 2\ 2]^{\mathrm{T}}$ m, $\mathbf{r}^{(2)} = [0\ 3\ 2]^{\mathrm{T}}$ m, and $\mathbf{r}^{(3)} = [0\ 1\ 2]^{\mathrm{T}}$ m and the desired formation uses the equations (39-42) but with $\tau = 1$ m and $\eta = 0$ m. Figure 11 adds lateral disturbance force F_y only in the vehicle 3 and provides that a safe distance between vehicles are now $\mathbf{D} = [0\ 0.95\ 0]^{\mathrm{T}}$ m. It is observed that when the vehicle 3 moves due to disturbance applied, the vehicle 1 also moves proportionally to meet the safety distance $\mathbf{D}$. It is noted that at this time, the coordinates of the longitudinal axis r_x of the three vehicles remains the same. The altitude of the vehicles 1 and 2 undergoes a little variations relative to the altitude reference because in the moment that the vehicle undergoes the disturbance, the engines turn faster generating more thrust to keep the vehicles in the desired position.

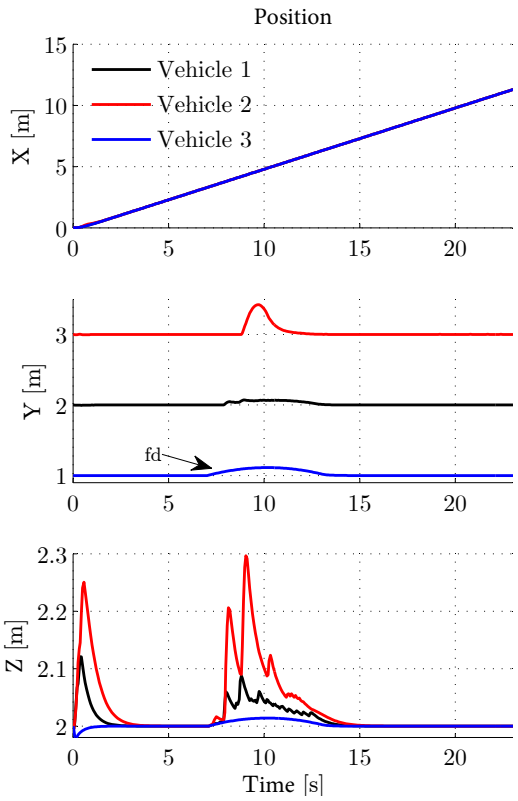

Fig. 11. Collision avoidance constraint acting in the vehicles 1 e 2 when vehicle 3 undergoes disturbance

V. Conclusions

This article discussed the problem of adding position constraints to the formulation from a multirotor position control, so as to ensure collision avoidance. The problem was solved using standalone controllers based on a predictive controller with a simple linear quadratic formulation. The method was evaluated through computer simulations considering that the vehicle was subjected to lateral disturbances forces to cause change in the formation. It is concluded that the proposed method was able to reject these disturbances to a certain limit of lateral force magnitude, making this method a good solution for multirrotor formation control in indoor environment. For a future work, different types of formations will be investigated and a hardware-in-the-loop (HIL) environment will be used for experimental evaluation of the proposed method.

Acknowledgment

The authors would like to thank the Conselho Nacional de Desenvolvimento Científico e Tecnológico (CNPq) and the Instituto Tecnológico de Aeronáutica (ITA) by the necessary support to realize the present work.

REFERENCES

[1] A. Ryan, M. Zennaro, A. Howell, R. Sengupta, J. K. Hedrick. An Overview of Emerging Results in Cooperative UAV Control, *Proceedings of IEEE Conference on Decision and Control*, Atlantis, Paradise Islands, Bahamas, 2004.

[2] T. Schouwenaars, E. Feron, J. How. Multi-vehicle path planning for non-line of sight communication, *Proceedings of the American Control Conference*, 2006.

[3] D. Mellinger, A. Kushleyev, V. Kumar. Mixed-Integer Quadratic Program Trajectory Generation for Heterogeneous Quadrotor Teams, *Proceedings of the 2012 IEEE International Conference on Robotics and Automation*, Saint Paul, Minnesota, United States, 2012.

[4] Z. Chao, L. Ming, Z. Shaolei, Z. Wenguang. Collision-free UAV Formation Flight Control based on Nonlinear MPC, *Proceedings of the 2011 IEEE International Conference on Electronics, Communications and Control*, Ningbo, 2011.

[5] I. A. A. Prado, D. A. Santos. Multirotor position tracking using a linear constrained model predictive controller, *22nd International Congress of Mechanical Engineering*, Ribeiro Preto, SP, 2013.

[6] D. A. Santos, O. Saotome, A. Cela. Trajectory control of multirotor helicopters with thrust vector constraints. In: 2013 21st Mediterranean Conference on Control & Automation (MED), 2013, Platanias. 21st Mediterranean Conference on Control and Automation, 2013. p. 375.

[7] J. Yan, D. A. Santos, D. S. Bernstein. Adaptive Control with Convex Saturation Constraints. In: Dynamic Systems and Control Conference, 2013, Palo Alto. Proceedings of the ASME 2013 Dynamic Systems and Control Conference, 2013.

[8] I. A. A. Prado, D. A. Santos. A Safe Position Tracking Strategy for Multirotor Helicopters, *22th Mediterranean Conference on Control and Automation (MED)*, Palermo, Italy, 2014.

[9] J. M. Maciejowski. Predictive Control with Constraints. Harlow: Prentice-Hall, 2002.

[10] M. Shuster, A Survey of Attitude Representations, *The Journal of the Astronautical Sciences*, 41(4), 1993, 439-517.

[11] K. Nonami, F. Kendoul, S. Suzuki, W. Wang, D. Nakazawa. Autonomous Flying Robots: Unmanned Aerial Vehicles and Micro Aerial Vehicles. Springer, 2010.